HHS Public Access

Author manuscript

Ultrasound Med Biol. Author manuscript; available in PMC 2020 February 01.

Published in final edited form as:

Ultrasound Med Biol. 2019 February ; 45(2): 429–439. doi:10.1016/j.ultrasmedbio.2018.08.019.

Quantitative ultrasound biomarkers based on backscattered acoustic power: potential for quantifying remodeling of the human cervix during pregnancy

Quinton W. Guerrero[a], **Helen Feltovich**[a,b], **Ivan Rosado-Mendez**[a], **Lindsey C. Carlson**[a,b], and **Timothy J. Hall**[a,*]

[a]Medical Physics Department, University of Wisconsin, Madison, Wisconsin 53705

[b]Maternal Fetal Medicine Department, Intermountain Healthcare, Provo, Utah 84601

Abstract

As pregnancy progresses, the cervix remodels from a rigid structure to one compliant enough to allow delivery of a fetus, a process which involves progressive disorganization of cervical microstructure. Quantitative ultrasound biomarkers that may detect this process include those derived from the backscattered echo signal, namely, acoustic attenuation and backscattered power loss. We have recently shown that attenuation and backscattered power loss are affected by tissue anisotropy and heterogeneity in the ex vivo cervix. In this study, we compared attenuation and backscattered power difference in a group of women in early (first trimester), to a group in late (third trimester), pregnancy. We found a significant decrease in the backscattered power difference in late as compared to early pregnancy, suggesting decreased microstructural organization in late pregnancy, a finding that is consistent with animal models of cervical remodeling. In contrast, we found no difference in attenuation between the timepoints. These results suggest that the backscattered power difference, but perhaps not attenuation, may be a useful clinical biomarker of cervical remodeling.

Keywords

Ultrasound backscatter; Anisotropy; Cervix

Introduction

By the end of pregnancy, the normal cervix has remodeled from a rigid structure strong enough to maintain a growing fetus in utero to one compliant enough to allow that fetus to deliver. Cervical softening is digitally palpable by 6–8 weeks of gestation (Danforth, 1983) and softness is one parameter used by clinicians to evaluate readiness of the cervix for

*Corresponding Author: Timothy J. Hall, 1111 Highland Ave, Medical Physics De-partment, University of Wisconsin, Madison, Wisconsin 53705; tjhall@wisc.edu; Phone, 608-265-6116.

delivery. Invasive study in women is impractical, but animal models reveal that this softening process involves progressive disorganization of cervical microstructure (Word et al., 2007; Myers et al., 2015; Akins et al., 2011).

Premature cervical change can lead to preterm birth (Feltovich, 2017), a significant obstetrical problem that affects ~10% of pregnancies (Chang et al., 2013). Unfortunately, our ability to predict and prevent this is poor because by the time the cervix is short or the uterus is regularly contracting, it is often too late; this is why it is estimated that even if all pregnant women were screened and offered appropriate available clinical intervention, 95% of preterm births would still occur (Chang et al., 2013). In fact, despite intense research efforts, the preterm birth rate has been rising in recent years (Martin et al., 2015). The opposite problem, post-term birth, is also significant because its associated risk of stillbirth leads to increased resource utilization due to unsuccessful elective labor induction (Spong et al., 2012). The primary issue is that the decision to induce labor is based upon cervical "favorability" but there is no consistent definition of the favorable cervix (Spong et al., 2012). The most common metric used in clinical practice, the Bishop score, is antiquated and inappropriate; it was designed in the 1960s (Bishop, 1964) to predict which multiparous women were most likely to labor in the near future. The score was based on digital assessment of cervical dilation, length, softness, position, and proximity of the fetal head to the cervix. While a higher score did correlate with a shorter time before labor spontaneously began (Bishop, 1964), the important point is that the score was not developed for prediction of induction success, especially among nulliparous women, yet is used routinely for this purpose because there is no good alternative (Crane, 2006; Saccone et al., 2016). Unsurprisingly, it is a poor predictor of induction success (Kolkman et al., 2013).

The ability to objectively quantify cervical evaluation could improve prediction of delivery (pre-or post-term) and facilitate comprehensive understanding of the remodeling process, which could in turn elucidate novel targets for therapies to prevent abnormal timing. For this reason, noninvasive quantitative ultrasound (QUS) techniques for evaluating the cervix are currently under investigation (Carlson et al., 2015; Hernandez-Andrade et al., 2013; Molina et al., 2012; Muller et al., 2015; Peralta et al., 2015; McFarlin et al., 2010, 2006a, 2015a,b; Labyed et al., 2011; Feltovich et al., 2012; Carlson et al., 2014a,b, 2015; Guerrero et al., 2018; Huang et al., 2016; Feltovich et al., 2010; McFarlin et al., 2006b).

Acoustic attenuation is one QUS parameter that has been proposed as a biomarker of microstructural reorganization (Bigelow et al., 2008). Mc-Farlin et al. have shown in pregnant women that a parameter based on the backscattered echo signal, the specific attenuation coefficient (SAC), decreases as gestational age increases (McFarlin et al., 2010). Unfortunately,the inter-subject variability of this parameter is as great as the difference expected from early to late gestation (McFarlin et al., 2010, 2015a), which of course limits its clinical usefulness. One potential explanation for the high variability is that anisotropy and spatial heterogeneity were not evaluated. This can be problematic because violating the assumptions of isotropy and homogeneity may lead to erroneously high variances in tissues with highly aligned microstructure (Nassiri et al., 1979). For example, violating the assumption of anisotropy in a clearly anisotropic tissue such as striated muscle would be inappropriate; this has been demonstrated in both skeletal muscle (Nassiri et al., 1979; Topp

and O'Brien, 2000) and cardiac muscle (Mottley and Miller, 1990; Milne et al., 2012; Hoffmeister et al., 1995). One might reasonably assume that the same principle would apply to the cervix because human (Danforth, 1983; Reusch et al., 2013; Weiss et al., 2006) and animal (Word et al., 2007; Mahendroo, 2012) studies alike demonstrate that the cervix contains pseudo-aligned layers of collagen, dominated by a central circumferential band. Further, this microstructure actively remodels during pregnancy, as demonstrated with nonlinear optical microscopy (Akins et al., 2010) (see Figure 1) and fluorescence microscopy (Feltovich et al., 2005) in rodent models. Given this probable anisotropy, one might expect the SAC to show anisotropy, in other words, demonstrate angle-dependence of acoustic properties. In fact, it does; we have recently demonstrated in cervical tissue that the SAC, and a related parameter based on the backscattered echo signal, the mean backscattered power difference (*m*BSPD), demonstrate anisotropy (Guerrero et al., 2018).

In addition, violating the assumption of spatial homogeneity could lead to erroneously high variances. One might expect spatial heterogeneity to affect QUS measurements in the cervix because the microstructural layers gradually change from proximal to distal (Carlson et al., 2015; Weiss et al., 2006). In fact, we have recently confirmed that spatial variability in the cervix does affect both the SAC and *m*BSPD (Guerrero et al., 2018).

In summary, our recent findings suggest that anisotropy and spatial heterogeneity, in both the cervical tissue itself and QUS parameters that describe it, should not be ignored. These findings motivated us to explore attenuation and backscattered power difference as potential biomarkers of cervical remodeling in pregnant women, controlling for anisotropy and spatial heterogeneity by acquiring data from a consistent location in the mid cervix with a linear array transducer. We chose a linear array for tight control over the angle of incidence of the acoustic beam; previous studies used a curved-linear array, which may increase measurement variability because it provides continuously-varying angle of incidence between the acoustic beams and tissue, as opposed to all beams interacting at the same angle of incidence. We studied a group of women in early pregnancy (first trimester, 1T) and another group in late pregnancy (third trimester, 3T). The aims of our study were to determine whether we could reduce the variance in attenuation estimates compared to those reported by McFarlin et al. (2010, 2015b), whether there was a significant difference in attenuation estimates in the cervix for early versus late pregnancy in women, whether the angle-dependence of backscattered power found in the *ex vivo* cervix would be present *in vivo*, and whether that parameter changed as might be expected based on Fig. 1.

Materials and Methods

Patient Recruitment

Thirty-six pregnant women participated in this cross-sectional study, all of whom provided written informed consent. The study was approved by the institutional review boards at the University of Utah and the University of Wisconsin. Sixteen (n=16) of the women were presenting for termination of pregnancy in the first trimester (5–14 weeks gestation), and 20 for induction of labor at term in the third trimester (37–41 weeks) and underwent the ultrasound exam before their procedure as described by Carlson et al. (2018). Table 1 describes the entire cohort.

Data Acquisition and Processing

To reduce interobserver variability, all acquisitions were overseen by the same engineer (L.C.C.), and all exams in each group of women done by the same clinician (H.F. for 3T exams, and Dr. Stephanie Romero for 1T). We used a Siemens Acuson S3000 ultrasound system (Siemens Healthcare, Ultrasound Business Unit, Mountain View, CA, USA). Radiofrequency (RF) echo signal data was acquired with a prototype catheter transducer (128 elements, 14 mm aperture, 3 mm diameter) operated in linear array mode (at a nominal frequency of 10 MHz) to allow for parallel acoustic A-lines when beamsteering.

The prototype transducer was secured to the index finger of the clinician's hand, with the active aperture on her fingertip, and placed in a sterile glove filled with acoustic coupling gel (Carlson et al., 2015). Her finger was placed roughly parallel to the endocervical canal, midway along the length of the cervix on the anterior (3T) or posterior (1T) cervix (see Figures 2(a)-(b)). This location was based upon results from *ex vivo* studies of both SWS and QUS backscatter parameters in the human cervix (Carlson et al., 2014a; Guerrero et al., 2018) and logistics (the anterior 1T cervix is difficult to access). Location was verified with B-mode ultrasound prior to RF data acquisition.

We used the Axius Direct Ultrasound Research Interface (Brunke et al., 2007) to acquire two sets of beamsteered RF echo signal data during the exam in 1T women, and one set during the exam in the 3T women. Fifteen independent frames of RF echo signal data were collected as acoustic beams were steered from −28° to +28° in steps of 4°. All RF echo signal data were sampled at 40 MHz. The data was downloaded and analyzed off-line using MATLAB (Mathworks, Natick, MA, USA).

As described in Guerrero et al. (2017), we used the Reference Phantom Method (Yao et al., 1990) to account for system effects on the backscatter echo signal power spectrum. This approach is well established in the literature for providing system-independent estimates of attenuation and scattering properties by accounting for diffraction characteristics and system behavior (Nam et al., 2012, 2013; Rosado-Mendez et al., 2013). Specifically, after the exam, 10 sets of 15 beamsteered RF frames were collected from one of two reference phantoms. The reference phantom for the 1T study was composed of an agar gel containing graphite powder (50 g/L) and glass beads (4 g/L, 3000E beads; ~5–20 μm); Potter's Industries, Malvern, PA, USA). It had a speed of sound of 1560 m/s and a linear attenuation near 0.67 $dB{\cdot}cm^{-1}MHz^{-1}$ in the 2–10 MHz bandwidth and was housed in an acrylic container covered on one side with a 25 μm thick Saran (polyvinylidene chloride; Dow Chemical, Midland, MI, USA) scanning window. The reference phantom for the 3T study was homogeneously composed of an animal hide gelatin mixture containing graphite powder (30 g/L) and glass beads (4 g/L, 3000E beads, (5–20 μm); Potter's Industries, Malvern, PA, USA). It had a speed of sound of 1550 m/s, and a linear attenuation in the 2–10 MHz bandwidth of 1.51 $dB{\cdot}cm^{-1}MHz^{-1}$, and was housed in an acrylic cylinder covered on both sides with a 25 μm thick Saran (polyvinylidene chloride; Dow Chemical, Midland, MI, USA) scanning window.

Quantitative Ultrasound Parameter Estimation

Power Spectral Estimation—The bias and variance of QUS parameters depend on the size of the power spectral estimation region and parameter estimation region used (Rosado-Mendez et al., 2013). The multitaper method (Thomson, 1982) appears to be the optimal power spectral estimation method to reduce bias and variance of attenuation when restricting the size of the power spectral estimation region (Rosado-Mendez et al., 2013). Therefore, to choose the optimal power spectral estimation regions (PSER) and parameter estimation region (PER) sizes, we first followed the methods of Thijssen (2003) to measure the axial and lateral pulse echo correlation length of the prototype probe (247 μm and 330 μm respectively). Then, based upon our estimated correlation lengths and previous results (Rosado-Mendez et al., 2013), we determined that a 4×4 mm power spectral estimation region, a 10×4 mm attenuation PER, and a 4×4 mm BSPD PER were optimal for QUS parameter estimation.

Backscattered Power Parameter Estimation—The mean backscattered power difference (*m*BSPD), which quantifies the angle-dependence of backscattered power, was estimated as previously described (Guerrero et al., 2017, 2018). Briefly, power spectra of RF echo signals are measured at an equivalent depth in the sample media and reference phantom that has only spherical scattering sources (for angle-independent backscatter). A usable bandwidth is defined and the log ratio of sample to reference phantom power spectra in the usable bandwidth averaged (the backscattered power difference (BSPD)). The BSPD is estimated among all beamsteering angles to identify the angle at which the maximum BPSD occurs (the ‘normalization angle’; θ_{norm}). The value of the maximum BSPD is then subtracted from all other BSPD estimates in the beamsteering range (the ‘normalized BSPD’ (nBSPD); see Figs. 3 and 4 of Guerrero et al. (2017)). This parameter describes the backscattered power as a function of beam-steering angle relative to both the reference phantom and the angle of highest BSPD. The average nBSPD among all beamsteering angles is the mean BSPD (*m*BSPD). The *m*BSPD quantifies the angle-dependence of backscattered power, and is related to the magnitude of anisotropy in the underlying scattering structure.

Angular Range—There is a trade-off in the angular range selected for analysis and the maximum axial depth and lateral extent shared by all beamsteering angles in parameters which quantify the angle-dependence of acoustic properties (Guerrero et al., 2018). This is shown in Figure 3, which demonstrates the shared area among all beamsteering angles as a function of angular range for the prototype linear array transducer geometry. We chose a ±28° beam-steering range because it is the largest angular range that extended to the average axial depth of the anterior and posterior cervix (~1.4 cm).

Attenuation Estimation—The specific attenuation coefficient (IEC 61391–2: 2010, 2010) was estimated using the Reference Phantom Method (Yao et al., 1990). This method relies on a calibrated reference phantom, composed homogeneously of spherical scatterers, to compensate for the system-dependence of RF echo signals and thus allow estimation of a tissue’s acoustic properties. Power spectra from the sample media and reference phantom RF echo signal are estimated at an equivalent depth, and the ratio of the power spectrum of

sample versus reference phantom determined. The attenuation coefficient is then estimated by a linear least-squares fit of the logarithm of the power spectral ratio versus depth at each frequency in the usable bandwidth. Most commonly, a linear fit is applied to the frequency-dependence of attenuation coefficient estimates in the bandwidth and the specific attenuation coefficient (SAC, also known as attenuation slope) reported in $dB \cdot cm^{-1} MHz^{-1}$. In our study, the SAC was estimated using a 5 MHz bandwidth (4–9 MHz). This lower frequency range, compared to the 10MHz center frequency of our excitation pules, is due to the relatively high SAC of the cervix (McFarlin et al., 2010).

Similar to our *ex vivo* study of the human cervix (Guerrero et al., 2018), we attempted to correct for the angle-dependence of the SAC by estimating the SAC at the normalization angle. Ideally, the normalization angle is the angle of normal incidence with an underlying aligned structure (Guerrero et al., 2017), and the SAC estimated at this angle minimizes the estimate bias due to anisotropy. To determine if accounting for anisotropy decreases inter-subject variability of the SAC, we compared SAC estimates made at the 0° beamsteering angle (SAC(0°)) to SAC estimates made at the normalization angle(SAC(θ_{norm})).

Region of Interest Selection—For each subject, the anterior or posterior cervix was demarcated on the B-mode image and all QUS parameter estimates not completely containing cervix tissue were excluded from analysis. Figure 4 shows the ROI for QUS parameter analysis in a B-mode image of a cervix. Due to the limited lateral extent of the transducer, QUS parameters were estimated beginning 2 mm from the transducer face (less that the 2.5mm elevation aperture length).

Bulk Motion Identification and Subject Removal—We used the Axius Direct Ultrasound Research Interface to acquire echo signal data. RF echo signal beamsteering acquisition for the ±28° angular range took approximately 30–50 sec and thus the data were vulnerable to bulk motion artifacts due to subject and/or clinician movement. Each exam (consisting of the beamsteered RF echo signal data) was therefore converted into a .gif movie of 15 B-mode images so that each dataset could be carefully evaluated for bulk motion artifacts. If artifacts were apparent, the data were removed from further analysis. In total, 13 examinations were removed from our analysis, as shown in Table 1.

Quantitative Ultrasound Parameter Statistics—We used a non-parametric two-way Wilcoxon Rank-Sum test, because it does not assume normally-distributed data and is more powerful than a standard two-way analysis of variance (ANOVA) test (Hollander et al., 2015). We used a 5% threshold for statistical significance between groups.

Results

Measures of Anisotropy

The *m*BSPD was significantly reduced from early (1T) to late (3T) pregnancy (average −0.90 dB from 1T to 3T; $p<0.05$). Box plots of *m*BSPD in early versus late pregnancy are shown in Figure 5. Median and IQR for the *m*BSPD in women in early and late pregnancy are summarized in Table 2.

Attenuation

Box plots of the SAC(0°) and SAC(θ_{norm}) of early (1T) and late (3T) groups are shown in Figure 6. A nonstatistically significant decrease in both SAC(0°) and SAC(θ_{norm}) was noted from 1T to 3T (average 0.06 and 0.07 dB·cm^{-1}MHz^{-1} for SAC(0°) and SAC(θ_{norm}) respectively from 1T to 3T; p=0.62 and p=0.78 for SAC(0°) and SAC(θ_{norm}) respectively). Median and IQR for the SAC(0°) and SAC(θ_{norm}) among 1T and 3T women are summarized in Table 2.

Discussion

We found that the mean backscattered power difference (*m*BSPD), but not the specific attenuation coefficient (SAC), distinguished the early (1st trimester) from the late (3rd trimester) cervix in pregnant women. Specifically, in early pregnancy, the *m*BSPD was 0.90 dB higher than in late pregnancy, a difference that was statistically significant. Unexpectedly, even when anisotropy and spatial heterogeneity were taken into account, there was no difference in the SAC between the two timepoints. To our knowledge, this is the first study of anisotropy and spatial heterogeneity in the cervix of pregnant women.

We were not surprised by the *m*BSPD results because higher values are expected from a tissue whose microstructure is highly organized and aligned. For example, *m*BSPD is greater in an anisotropic tissue or medium, namely, bicep muscle imaged longitudinally or phantom containing rod-like aligned scatterers, as compared to a relatively isotropic tissue or medium, namely, bicep muscle imaged in the transverse plane or phantom containing randomly placed spheres (Guerrero et al., 2018). Our findings that *m*BSPD is greater in the early, as compared to the late, pregnant cervix, which suggests that the microstructure is more highly organized and aligned in early pregnancy, is consistent with animal models that indicate progressive disorganization of cervical microstructure during gestation (Word et al., 2007; Akins et al., 2010, 2011; Mahendroo, 2012; Myers et al., 2015).

Contrary to our expectations, however, the SAC values showed even greater inter-subject variability than that reported in previous studies (McFarlin et al., 2010, 2015a,b). We hypothesized that refining the estimate by accounting for anisotropy and spatial heterogeneity, and using a linear (as opposed to a curved-linear) transducer, would reduce inter-subject variability and make the estimates more robust. This was not the case, despite that we acquired data with the linear transducer from a consistent location along the cervix (to control for spatial variability) and estimated the SAC at the nor-malization angle (to control for anisotropy). Specifically, for both SAC(0°) and SAC(θ_{norm}) estimates from our early pregnancy group, the inter-subject variability (reported as the standard deviation of the SAC among individual women) were ±0.64 and ±0.69 dB·cm^{-1}MHz^{-1} for SAC(0°) and SAC(θ_{norm}) respectively. This is higher than that observed in a study of women at any trimester of pregnancy, in which anisotropy and spatial heterogeneity were not considered, and data was acquired with a curved-linear transducer (standard deviation of ±0.36 dB·cm^{-1}MHz^{-1}(McFarlin et al., 2010)). Further, the inter-subject variability in our late pregnancy group (standard deviation of ±1.07 and ±1.24 dB·cm^{-1}MHz^{-1} for SAC(0°) and SAC(θ_{norm}) respectively) was higher than previously reported in a study of women in late pregnancy (standard deviation of ±0.4 dB·cm^{-1}MHz^{-1} (McFarlin et al., 2015a)). This raises the

possibility that the issue may not be the parameter itself, but instead the property it measures. Specifically, it is presumed that attenuation depends on hydration status of the cervix, and that hydration increases as gestation progresses (Bigelow et al., 2008; McFarlin et al., 2015b). This is not unreasonable; recent studies in pregnant women confirm that as pregnancy advances, cervical diameter and volume increase (Andrade et al., 2017) as does surface area (Qian et al., 2016). Interestingly, these observations are not consistent with tissue biopsies, which demonstrate a relatively small difference (3–6%) in hydration between the early (or non-) pregnant cervix and late pregnant cervix (Uldbjerg et al., 1983; Danforth et al., 1974; Petersen and Uldbjerg, 1996; Rechberger et al., 1988). An optical technique (frequency-domain near-infrared spectroscopy, FD-NIRS), found no difference in cervical hydration in early, as compared to late, pregnancy (Hornung et al., 2011). In other words, it appears that cervical hydration does not change markedly during pregnancy, which might explain why we did not find attenuation to be a useful biomarker in this study.

This study has limitations. One is its small size. It was powered only to determine if a difference in QUS parameter values could be detected in early versus late pregnancy, and therefore the numbers are much too small to establish a nomogram or cutoff values at any particular gestational age. Also, the ability of others to reproduce our results is limited because we used a cumbersome prototype transducer that was designed for a different purpose (intravascular imaging). Further, its small aperture (1.4 cm) meant that we could only evaluate a small area of the cervix and also that the size of the shared area among all beamsteered angles was small, which reduced the number of independent estimates of the angle-dependence of backscattered power. Also, the length of time required for data acquisition (30–50 seconds) meant that more than 1/3 of the data had to be discarded because of bulk motion. To address these concerns, we have a new prototype linear array transducer that has a larger aperture and better data collection software. This allows a greater number of independent A-lines used in power spectral estimation, which should reduce inter-subject variability. Although the clinical usefulness of this study is limited by its small size, the positive results prompted us to continue the investigation in a larger group of women, with the new transducer. Specifically, we are currently conducting a longitudinal study in pregnant women in which we measure both backscattered power difference and shear wave speed throughout gestation to quantify cervical microstructural disorganization and resultant softening, respectively. The ability to precisely describe cervical remodeling in pregnancy should lead to a comprehensive understanding of the process, which could in turn lead to targeted studies of abnormal birth timing such as preterm or post-dates birth.

Conclusions

We found that the mean backscattered power difference (*m*BSPD), but not the specific attenuation coefficient (SAC), distinguished the early (1st trimester) from the late (3rd trimester) pregnant cervix in a group of women from each timepoint. Unexpectedly, we also found that acoustic attenuation estimates had high variance even after accounting for anisotropy and spatial heterogeneity. Although the difference in *m*BSPD was statistically significant, this study was powered only to explore whether differences in QUS parameter values could be detected in early versus late pregnancy, and therefore numbers were too small to establish a nomogram or cutoff values at any particular gestational age. Larger

studies are needed to clarify whether QUS parameters can be clinically useful biomarkers of cervical remodeling.

Acknowledgements

The authors would like to thank Dr. Stephanie Romero, who assisted with some of the ultrasound exams, as well as Prof. Ernest Madsen and Gary Frank, who constructed the phantoms. We are also grateful for the technical support from Siemens Ultrasound. Research reported here was supported by National Institutes of Health Grants T32CA009206 from the National Cancer Institute and R21HD061896, R21HD063031, and R01HD072077 from the Eunice Kennedy Shriver National Institute of Child Health and Human Development. The content is solely the responsibility of the authors and does not necessarily represent the official views of the National Institutes of Health.

References

Akins ML, Luby-Phelps K, Bank RA, Mahendroo M. Cervical softening during pregnancy: regulated changes in collagen cross-linking and composition of matricellular proteins in the mouse. Biol. Reprod, 2011;84:1053–1062. [PubMed: 21248285]

Akins ML, Luby-Phelps K, Mahendroo M. Second harmonic generation imaging as a potential tool for staging pregnancy and predicting preterm birth. J Biomed Opt, 2010;15:026020. [PubMed: 20459265]

Andrade KC, Bortoletto TG, Almeidal CM, Daniel RA, Avo H, Pacagnella RC, Cecatti JG. Reference ranges for ultrasonographic measurements of the uterine cervix in low-risk pregnant women. Rev Bras Ginecol Obstet, 2017;39:443–452. [PubMed: 28778109]

Bigelow TA, McFarlin BL, O'Brien WD, Oelze ML. In vivo ultrasonic attenuation slope estimates for detecting cervical ripening in rats: Preliminary results. J Acoust Soc Am, 2008;123:1794–1800. [PubMed: 18345867]

Bishop EH. Pelvic scoring for elective induction. Obstet Gynecol, 1964;24:266–268, [PMID:]. [PubMed: 14199536]

Brunke SS, Insana MF, Dahl JJ, Hansen C, Ashfaq M, Ermert H. An ultrasound research interface for a clinical system. IEEE Trans Ultrason Ferroelectr Freq Control, 2007;54:198–210. [PubMed: 17225815]

Carlson LC, Feltovich H, Palmeri ML, Dahl JJ, Munoz del Rio A, Hall TJ. Estimation of shear wave speed in the human uterine cervix. Ultrasound in Obstetrics & Gynecology, 2014a;43:452–458. [PubMed: 23836486]

Carlson LC, Feltovich H, Palmeri ML, Munoz del Rio A, Hall TJ. Statistical analysis of shear wave speed in the uterine cervix. Ultrasonics, Ferro-electrics, and Frequency Control, IEEE Transactions on, 2014b;61:1651–1660.

Carlson LC, Hall TJ, Rosado-Mendez IM, Palmeri ML, Feltovich H. Detection of changes in cervical softness using shear wave speed in early versus late pregnancy: An in vivo cross-sectional study. Ultrasound in medicine & biology, 2018;44:515–521. [PubMed: 29246767]

Carlson LC, Romero ST, Palmeri ML, Mu˜noz del Rio A, Esplin SM, Rotem-berg VM, Hall TJ, Feltovich H. Changes in shear wave speed pre-and post-induction of labor: a feasibility study. Ultrasound in Obstetrics & Gynecology, 2015;46:93–98. [PubMed: 25200374]

Chang HH, Larson J, Blencowe H, Spong CY, Howson CP, Cairns-Smith S, Lackritz EM, Lee SK, Mason E, Serazin AC, Walani S, Simpson JL, Lawn JE. Preventing preterm births: analysis of trends and potential reductions with interventions in 39 countries with very high human development index. Lancet, 2013;381:223–234. [PubMed: 23158883]

Crane JM. Factors predicting labor induction success: a critical analysis. Clin Obstet Gynecol, 2006;49:573, []. [PubMed: 16885664]

Danforth DN. The morphology of the human cervix. Clin Obstet Gynecol, 1983;26:7–13. [PubMed: 6839572]

Danforth DN, Veis A, Breen M, Weinstein HG, Buckingham JC, Manalo P. The effect of pregnancy and labor on the human cervix: changes in collagen, glycoproteins, and glycosaminoglycans. Am. J. Obstet. Gynecol, 1974;120:641–651. [PubMed: 4278606]

Feltovich H Cervical evaluation: from ancient medicine to precision medicine. Obstet Gynecol, 2017;130:51–63, [PMID:]. [PubMed: 28594774]

Feltovich H, Hall TJ, Berghella V. Beyond cervical length: emerging technologies for assessing the pregnant cervix. Am J Obstet Gynecol, 2012;207:345–354. [PubMed: 22717270]

Feltovich H, Ji H, Janowski JW, Delance NC, Moran CC, Chien EK. Effects of selective and nonselective pge2 receptor agonists on cervical tensile strength and collagen organization and microstructure in the pregnant rat at term. Am J Obstet Gynecol, 2005;192:753–760. [PubMed: 15746668]

Feltovich H, Nam K, Hall TJ. Quantitative ultrasound assessment of cervical microstructure. Ultrason Imaging, 2010;32:131–142. [PubMed: 20718243]

Guerrero QW, Feltovich H, Rosado-Mendez IM, Carlson LC, Li G, Hall TJ. Anisotropy and Spatial Heterogeneity in Quantitative Ultrasound Parameters: Relevance to Study of the Human Cervix. Ultrasound in Medicine & Biology, 2018; Accepted.

Guerrero QW, Rosado-Mendez IM, Drehfal LC, Feltovich H, Hall TJ. Quantifying backscatter anisotropy using the reference phantom method. IEEE Transactions on Ultrasonics, Ferroelectrics, and Frequency Control, 2017;64:1063–1077.

Hernandez-Andrade E, Hassan SS, Ahn H, Korzeniewski SJ, Yeo L, Chai-worapongsa T, Romero R. Evaluation of cervical stiffness during pregnancy using semiquantitative ultrasound elastography. Ultrasound Obstet Gynecol, 2013;41:152–161. [PubMed: 23151941]

Hoffmeister BK, Wong AK, Verdonk ED, Wickline SA, Miller JG. Comparison of the anisotropy of apparent integrated ultrasonic backscatter from fixed human tendon and fixed human myocardium. J Acoust Soc Am, 1995;97:1307–1313. [PubMed: 7876450]

Hollander MA Wolfe D, Chicken E. Nonparametric Statistical Methods John Wiley & Sons, Inc., 2015.

Hornung R, Spichtig S, Banos A, Stahel M, Zimmerman R, Wolf M. Frequency-domain near-infrared spectroscopy of the uterine cervix during regular pregnancies. Lasers Med Sci, 2011;26:205–212. [PubMed: 20814712]

Huang B, Drehfal LC, Rosado-Mendez IM, Guerrero QW, Palmeri ML, Simmons HA, Feltovich H, Hall TJ. Estimation of Shear Wave Speed in the Rhesus Macaques' Uterine Cervix. IEEE Trans Ultrason Ferroelectr Freq Control, 2016;63:1243–1252. [PubMed: 26886979]

IEC 61391–2: 2010. Ultrasonics Pulse-echo scanners Part 2: Measurement of maximum depth of penetration and local dynamic range. International Electrotechnical Commission, 2010.

Kolkman DG, Verhoeven CJ, Brinkhorst SJ, van der Post JA, Pajkrt E, Opmeer BC, Mol BW. The Bishop score as a predictor of labor induction success: a systematic review. Am J Perinatol, 2013;30:625–630, [PMID:]. [PubMed: 23283806]

Labyed Y, Bigelow TA, McFarlin BL. Estimate of the attenuation coefficient using a clinical array transducer for the detection of cervical ripening in human pregnancy. Ultrasonics, 2011;51:34–39. [PubMed: 20570308]

Mahendroo M Cervical remodeling in term and preterm birth: insights from an animal model. Reproduction, 2012;143:429–438. [PubMed: 22344465]

Martin JA, Osterman MJ, Kirmeyer SE, Gregory EC. Measuring Gestational Age in Vital Statistics Data: Transitioning to the Obstetric Estimate. Natl Vital Stat Rep, 2015;64:1–20.

McFarlin BL, Balash J, Kumar V, Bigelow TA, Pombar X, Abramowicz JS, O'Brien WD. Development of an ultrasonic method to detect cervical remodeling in vivo in full-term pregnant women. Ultrasound Med Biol, 2015a;41:2533–2539. [PubMed: 26004670]

McFarlin BL, Bigelow TA, Laybed Y, O'Brien WD, Oelze ML, Abramowicz JS. Ultrasonic attenuation estimation of the pregnant cervix: a preliminary report. Ultrasound Obstet Gynecol, 2010;36:218–225. [PubMed: 20629011]

McFarlin BL, Kumar V, Bigelow TA, Simpson DG, White-Traut RC, Abramowicz JS, O'Brien WD. Beyond cervical length: a pilot study of ultrasonic attenuation for early detection of preterm birth risk. Ultrasound Med Biol, 2015b;41:3023–3029. [PubMed: 26259887]

McFarlin BL, O'Brien WD, Oelze ML, Zachary JF, White-Traut RC. Quantitative ultrasound assessment of the rat cervix. J Ultrasound Med, 2006a;25:1031–1040. [PubMed: 16870896]

McFarlin BL, O'Brien WD, Oelze ML, Zachary JF, White-Traut RC. Quantitative ultrasound assessment of the rat cervix. J Ultrasound Med, 2006b;25:1031–1040. [PubMed: 16870896]

Milne ML, Singh GK, Miller JG, Holland MR. Echocardiographic-based assessment of myocardial fiber structure in individual, excised hearts. Ultrason Imaging, 2012;34:129–141. [PubMed: 22972911]

Molina FS, Gmez LF, Florido J, Padilla MC, Nicolaides KH. Quantification of cervical elastography: a reproducibility study. Ultrasound in Obstetrics & Gynecology, 2012;39:685–689. [PubMed: 22173854]

Mottley JG, Miller JG. Anisotropy of the ultrasonic attenuation in soft tissues: measurements in vitro. J Acoust Soc Am, 1990;88:1203–1210. [PubMed: 2229659]

Muller M, At-Belkacem D, Hessabi M, Gennisson JL, Grang G, Goffinet F, Lecarpentier E, Cabrol D, Tanter M, Tsatsaris V. Assessment of the cervix in pregnant women using shear waveelastography: A feasibility study. Ultrasound in Medicine & Biology, 2015;41:2789 – 2797. [PubMed: 26278635]

Myers KM, Feltovich H, Mazza E, Vink J, Bajka M, Wapner RJ, Hall TJ, House M. The mechanical role of the cervix in pregnancy. Journal of biomechanics, 2015;48:1511–1523. [PubMed: 25841293]

Nam K, Rosado-Mendez IM, Wirtzfeld LA, Ghoshal G, Pawlicki AD, Madsen EL, Lavarello RJ, Oelze ML, Zagzebski JA, O'Brien WD, Hall TJ. Comparison of ultrasound attenuation and backscatter estimates in layered tissue-mimicking phantoms among three clinical scanners. Ultrason Imaging, 2012;34:209–221. [PubMed: 23160474]

Nam K, Zagzebski JA, Hall TJ. Quantitative assessment of in vivo breast masses using ultrasound attenuation and backscatter. Ultrason Imaging, 2013;35:146–161. [PubMed: 23493613]

Nassiri DK, Nicholas D, Hill CR. Attenuation of ultrasound in skeletal muscle. Ultrasonics, 1979;17:230–232. [PubMed: 573006]

Peralta L, Mourier E, Richard C, Charpigny G, Larcher T, At-Belkacem D, Balla NK, Brasselet S, Tanter M, Muller M, Chavatte-Palmer P. In vivo evaluation of cervical stiffness evolution during induced ripening using shear wave elastography, histology and 2 photon excitation microscopy: Insight from an animal model. PLOS ONE, 2015;10:e0133377. [PubMed: 26317774]

Petersen LK, Uldbjerg N. Cervical collagen in non-pregnant women with previous cervical incompetence. Eur. J. Obstet. Gynecol. Reprod. Biol, 1996;67:41–45. [PubMed: 8789748]

Qian X, Jiang Y, Liu L, Shi S, Garfield R, Liu H. Changes in ectocervical surface area in women throughout pregnancy compared to non-pregnant and postpartum states. J Matern Fetal Neonatal Med, 2016;29:3677–3681. [PubMed: 26864001]

Rechberger T, Uldbjerg N, Oxlund H. Connective tissue changes in the cervix during normal pregnancy and pregnancy complicated by cervical incompetence. Obstet Gynecol, 1988;71:563–567. [PubMed: 3353047]

Reusch LM, Feltovich H, Carlson LC, Hall G, Campagnola PJ, Eliceiri KW, Hall TJ. Nonlinear optical microscopy and ultrasound imaging of human cervical structure. Journal of biomedical optics, 2013;18:031110–031110. [PubMed: 23412434]

Rosado-Mendez IM, Nam K, Hall TJ, Zagzebski JA. Task-oriented comparison of power spectral density estimation methods for quantifying acoustic attenuation in diagnostic ultrasound using a reference phantom method. Ultrason Imaging, 2013;35:214–234. [PubMed: 23858055]

Saccone GBS, Berghella V Transvaginal ultrasound cervical length for prediction of spontaneous labour at term: systematic review and meta-analysis. BJOG, 2016;123:16 – 22, [PMID:]. [PubMed: 26507579]

Spong C, Berghella V, Wenstrom K, Mercer B, Saade G. Preventing the first cesarean delivery: summary of a joint Eunice Kennedy Shriver National Institute of Child Health and Human Development, Society for Maternal Fetal Medicine, and American College of Obstetricians and Gynecologists Workshop. Obstet Gynecol, 2012;120:1182–1193, [].

Thijssen JM. Ultrasonic speckle formation, analysis and processing applied to tissue characterization. Pattern Recognition Letters, 2003;24:659–675.

Thomson DJ. Spectrum estimation and harmonic analysis. Proceedings of the IEEE, 1982;70:1055–1096.

Topp KA, O'Brien WD. Anisotropy of ultrasonic propagation and scattering properties in fresh rat skeletal muscle in vitro. J Acoust Soc Am, 2000;107:1027–1033. [PubMed: 10687711]

Uldbjerg N, Ekman G, Malmstrm A, Olsson K, Ulmsten U. Ripening of the human uterine cervix related to changes in collagen, glycosaminoglycans, and collagenolytic activity. American Journal of Obstetrics and Gynecology, 1983;147:662 – 666. [PubMed: 6638110]

Weiss S, Jaermann T, Schmid P, Staempfli P, Boesiger P, Niederer P, Caduff R, Bajka M. Three-dimensional fiber architecture of the nonpregnant human uterus determined ex vivo using magnetic resonance diffusion tensor imaging. Anat Rec A Discov Mol Cell Evol Biol, 2006;288:84–90. [PubMed: 16345078]

Word R, Li XH, Hnat M, Carrick K. Dynamics of cervical remodeling during pregnancy and parturition: Mechanisms and current concepts. Seminars in Reproductive Medicine, 2007;25:69–79. [PubMed: 17205425]

Yao LX, Zagzebski JA, Madsen EL. Backscatter coefficient measurements using a reference phantom to extract depth-dependent instrumentation factors. Ultrason Imaging, 1990;12:58–70. [PubMed: 2184569]

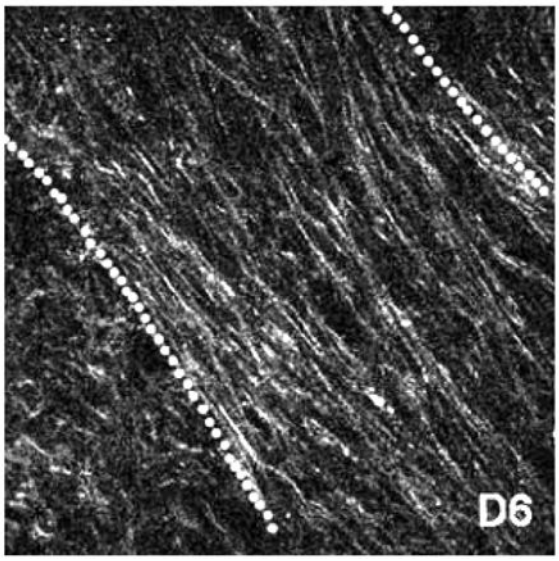

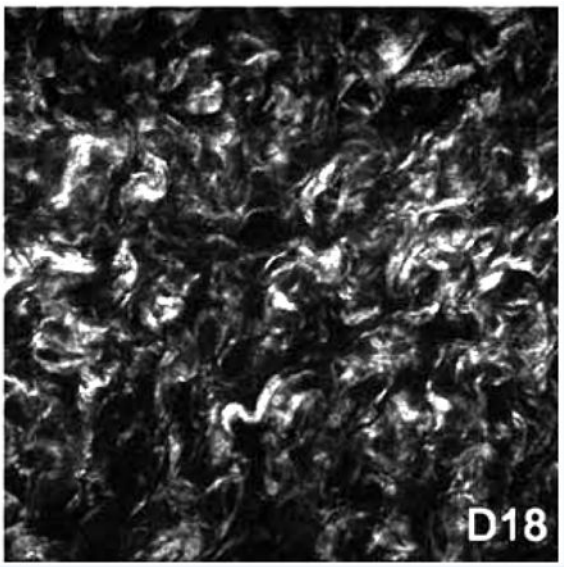

Figure 1:

Non-linear optical microscopy images of collagen fibers in the murine cervix at (a) day 6 and (b) day 18 pregnancy. This figure is reproduced from Figure 2 of Akins *et al., J. Biomed. Opt.*, 15(2):026020, 2010 and is reprinted with permission from SPIE and the authors.

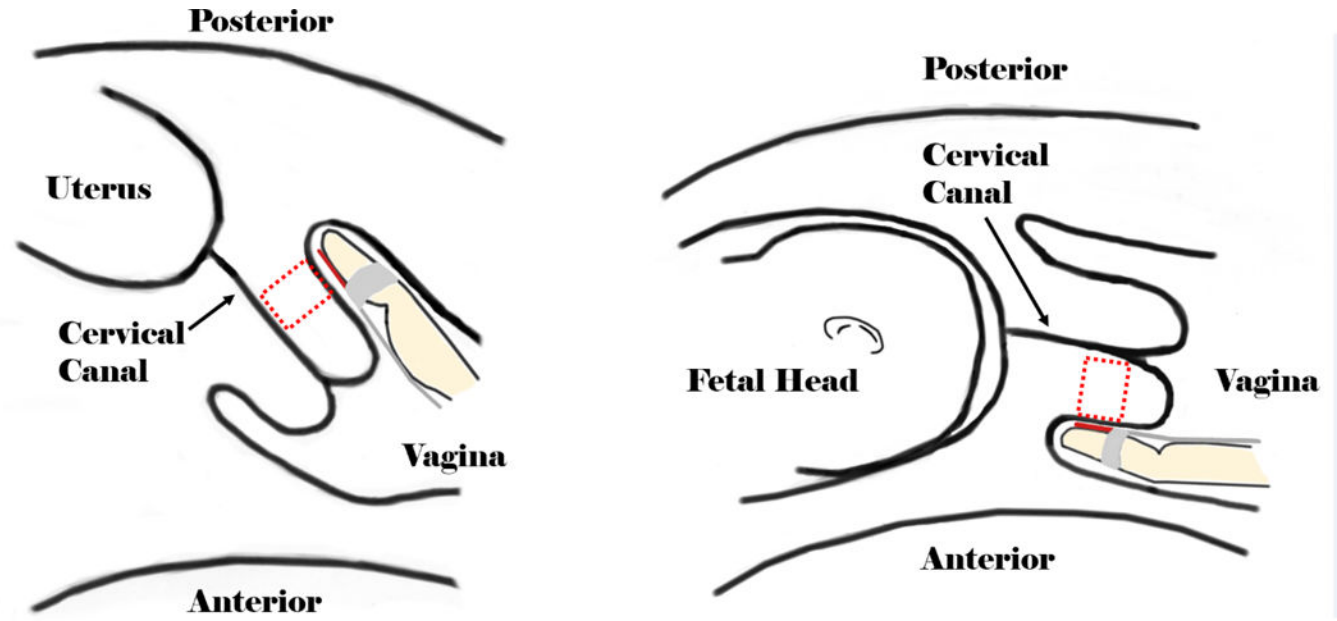

Figure 2:

Diagrams showing the experimental setup. The dashed boxes represent the approximate locations for ultrasound data acquisition.

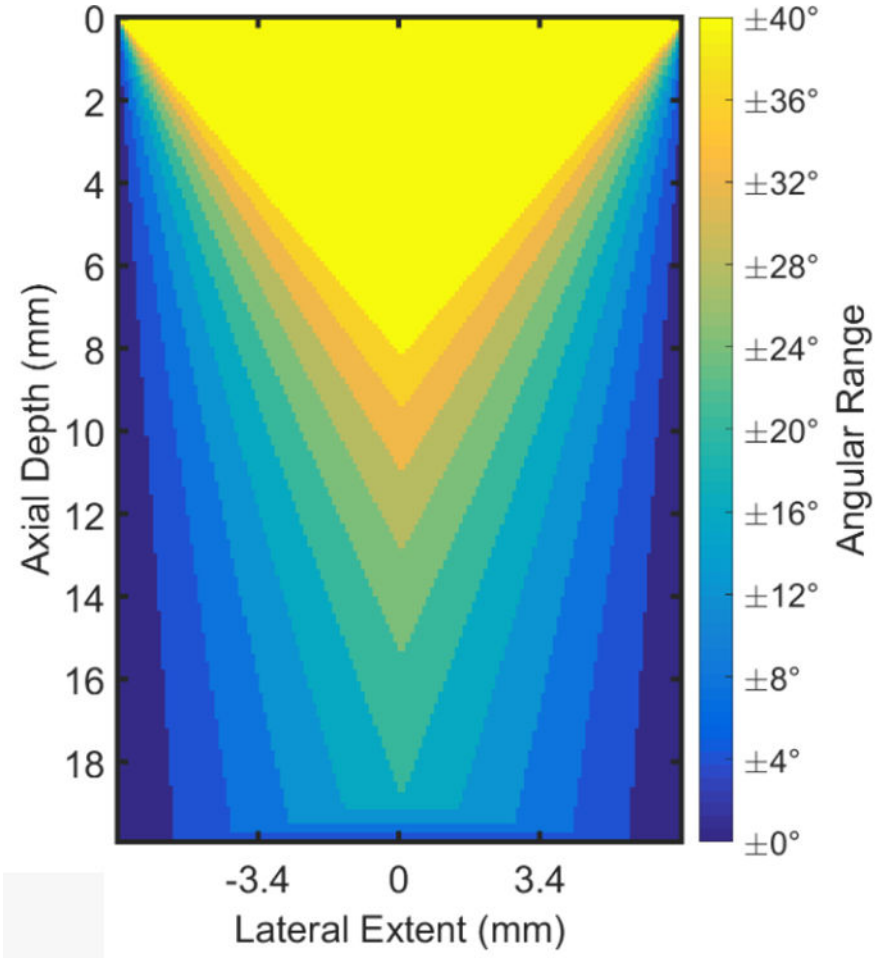

Figure 3:

A plot demonstrating the decrease in shared area among all beam-steering angles with increasing angular ranges for the prototype catheter transducer geometry. Lighter colors represent the wider range of angles, while darker colors represent fewer angles. We chose to use the ±28° angular range for our analysis.

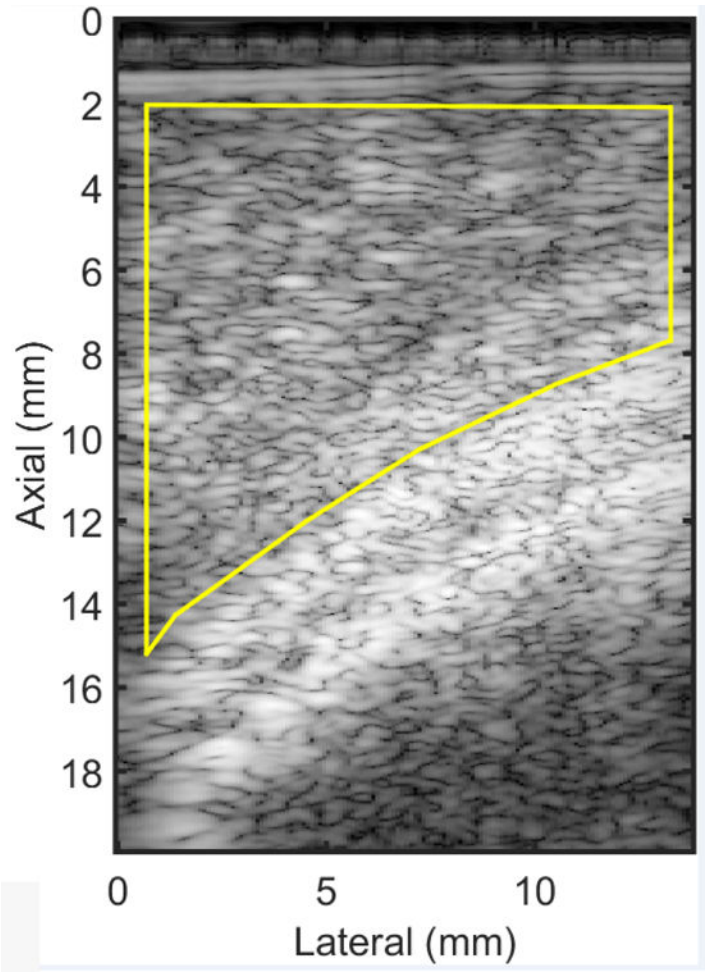

Figure 4:

An example B-mode image of a cervix from a woman in late pregnancy . The bright curved line that passes from left to right in the image is the fetal head. The solid yellow line demarcates the ROI for analysis; the anterior cervix.

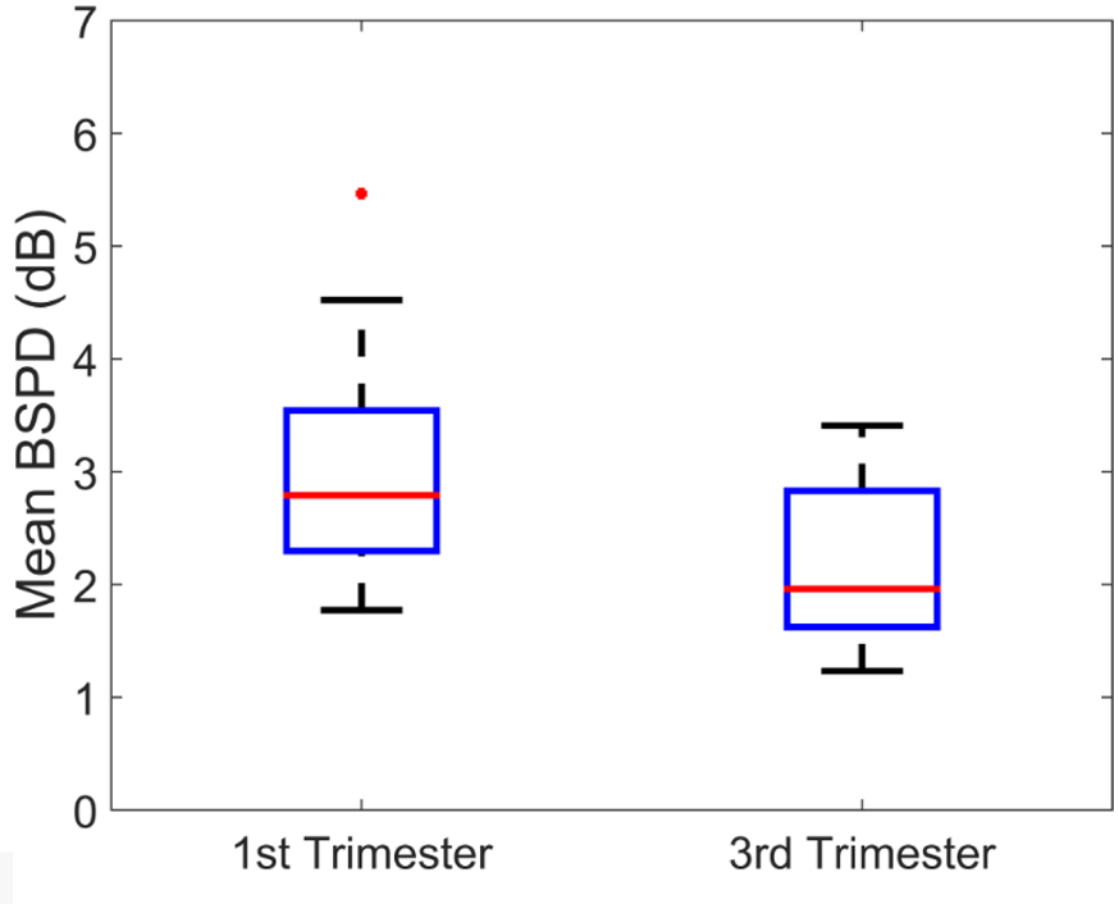

Figure 5:

Mean BSPD for early versus late pregnancy. The horizontal line near the middle of each box is the median value for that group, the boxes represent the interquartile range (IQR) among parameter estimates, the whiskers represent the maxima and minima within 1.5×IQR, and the dots are outliers outside of 1.5×IQR.

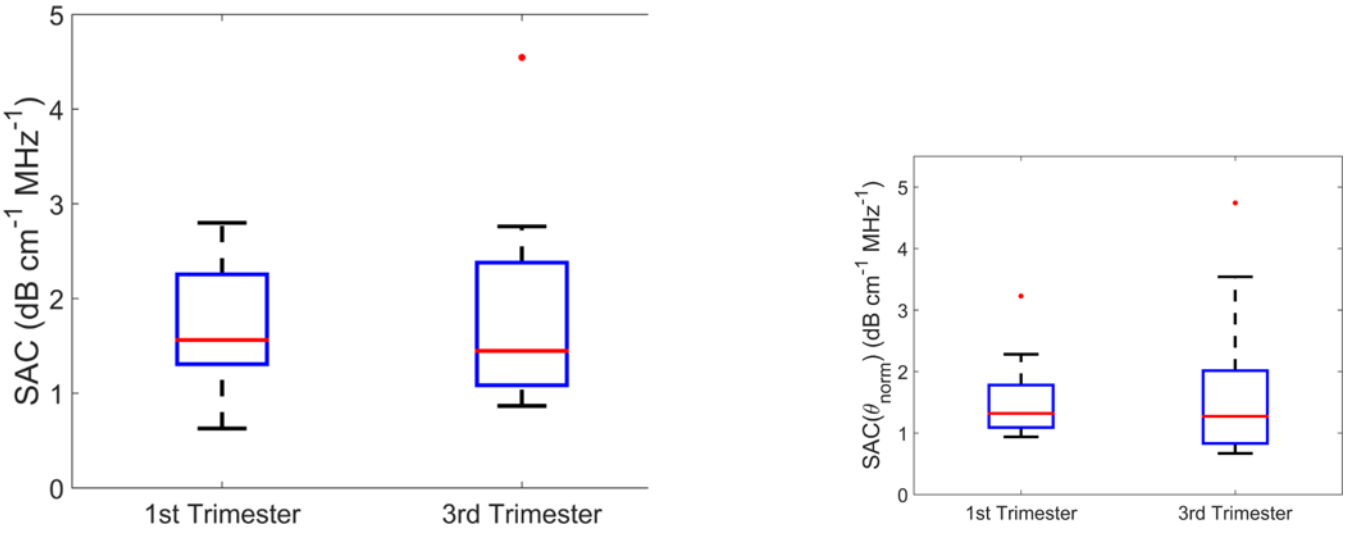

Figure 6:

The specific attenuation coefficient of the cervix estimated with acoustic beams at (a) the zero degree beamsteering angle (SAC(0°)) and (b) the normalization angle (SAC(θ_{norm})) for 1T versus 3T groups.

Table 1:

Group membership assignment for the entire cohort. (Bulk motion refers to subjects whose data was not analyzable due to evidence of bulk motion during the beamsteering RF echo signal acquisition process (see Methods).)

	Subjects Enrolled	Removed: Bulk Motion	Underwent Analysis
1T	16	5	11
3T	20	8	12

Table 2:

Median (95% Confidence Interval) for *m*BSPD and SAC estimates (estimated with acoustic beams at (0°) and (θ_{norm})) for 1T (first trimester) and 3T (third trimester) women from this study.

Trimester	*m*BSPD (dB)	SAC(0°) (dB·cm^{-1}MHz^{-1})	SAC(θ_{norm}) (dB·cm^{-1}MHz^{-1})
1T	2.79 (2.01 – 3.57)	1.71 (1.32 – 2.09)	1.32 (0.99 – 1.64)
3T	1.96 (1.41 – 2.51)	1.45 (0.86 – 2.03)	1.27 (0.74 – 1.81)